

Embedded Mesoporous Silica Silver Nanoparticles as potential antibacterial agent against Multidrug-Resistant Bacteria

¹Sanaa S. Zaki,²Kheiralla Z. H.,³Rushdy A. A.,⁴Betiha M.A. and ⁵Hanan B. Abousittash

1- Botany Department- Faculty of Women for Arts, Science and Education Ain Shams University, AsmaaFahmy,Cairo,Egypt

e-mail:sanaasobhy_2011@yahoo.com, e-mail:kheiralla@hotmail.com,e-mail:abeerahmedr@gmail.com, e-mail: habostash@gmail.com.

2- Egypt Refining Division, Egyptian Petroleum Research Institute, Cairo,Egypte-mail:Mohamed_betiha@hotmail.com

Abstract

Many workers have paid more attention to eco-friendly mesoporous silica silver nanoparticles featuring smaller particle sizes to enhance their remarkable antimicrobial properties. A simple chemical method was developed for synthesizing high valence silver nanoparticles immobilized on the mesoporous silica nanomaterial, which showed strong antibacterial activity. Chemical reduction of silver ion has been regarded in the present work, and a reducing agent, such as hydrazine was used to promote the reduction of the silver ion – precursor. The average particle size of the synthesized mesoporous silica-silver nanoparticles (Ag/NH₂-KIT-6(x)) with different concentrations of Ag (3.2 and 7.1%) calculated from Scherrer's equation for (1 1 1)-plane were 8 and 6.5 nm respectively. The synthesized materials were characterized using X-Ray diffraction (XRD), FTIR spectra, X-ray photoelectron spectroscopy (XPS) and transmission electron microscopy (TEM), which revealed the mesoporous silica nanoparticles.

Antibacterial activities of mesoporous silver nanoparticles against Gram-negative *Pseudomonas aeruginosa*(ATCC 9027) and Gram-positive *Staphylococcus aureus*(ATCC 43300) were found to be increased with the increasing of Ag concentration in the Ag/NH₂-KIT-6(x). The maximum inhibition zone diameter when the concentration 7.1 % was used obtained against *P. aeruginosa* and *S. aureus* with diameters of 32 and 30 mm respectively. The antimicrobial activity of mesoporous Ag/NH₂-KIT-6(x) was evaluated also using the MIC&MBC tests. The surface structures of both the untreated and the treated bacterial cells were examined by the aid of TEM. The treated bacterial cells were significantly changed, and major damage was observed in the outer cell membrane. In conclusion the use of AgNPs as antibacterial agent was found to be toxic against pathogenic bacteria and considered

Corresponding author:
e-mail: habostash@gmail.com

advantageous over other methods for control of pathogenic microorganisms, and it can be of great importance in developing novel drugs for curing many lethal diseases.

Key word: Mesoporous Silica-Silver Nanoparticles, Antimicrobial activity, Drug resistance

Introduction

Increasing hospital and community-acquired infections due to bacterial multidrug-resistant (MDR) pathogens for which current antibiotic therapies are not effective and represent a growing problem. Antimicrobial resistance and biofilm development in affected patients is thus one of the major threats to human health, since it determines an increase of morbidity and mortality as a consequence of the most common bacterial diseases (**Klevenset *et al.*, 2007 and Walker *et al.*, 2009**).

Mesoporous silica nanoparticles (MSNs) are well known for their biocompatibility, dispersibility, and chemical stability as carriers for drug/gene/antimicrobial agents. They have also been used as cell markers, catalytic substrates, absorbents, and matrix fillers (**Ruedas-Rama *et al.*, 2012; Yildirimet *al.*, 2013; Natarajan and Selvaraj, 2014 and Chen *et al.*, 2014**). They can be synthesized with controlled size, shape and varying textural properties (e.g. pore size, surface area and porosity) for therapeutic uses (**Wu *et al.*, 2013 and Qasimet *al.*, 2014**). Porous materials are of great interest because of their ability to interact with atoms, ions, molecules and nanoparticles not only at their surfaces, but throughout the bulk of the materials. Therefore, the presence of pores in nanostructured materials greatly promotes their physical and chemical properties (**Han *et al.*, 2011**).

Nanoparticles are now considered a viable alternative to antibiotics and seem to have a high potential to solve the problem of the emergence of bacterial multidrug resistance (**Raiet *al.*, 2012**). Metal nanoparticles of silver, copper, and gold have been found to be active against certain pathogenic bacteria and fungi. In particular, silver nanoparticles (AgNPs) have attracted much attention in the scientific field.

Silver has always been used against various diseases, in the past it was used as an antiseptic and antimicrobial against Gram-positive and Gram-negative bacteria (**Taraszkiewicz *et al.*, 2012 and Franciet *al.*, 2015**). Comparatively, AgNPs have been intensely studied owing to their distinct properties such as conductivity, chemical stability, catalytic activity, nonlinear optical behavior, low cytotoxicity and strong inhibitory and bactericidal effects as well as a broad spectrum of antimicrobial activities. These properties make them suitable for use as an antimicrobial agent in catheters, burns, severe chronic osteomyelitis, urinary tract infections and medical textiles.

Mesoporous silica AgNPs were considered, particularly attractive for the production of a new class of antimicrobials opening up a completely new way to combat a wide range of bacterial pathogens (**Sweet and Singleton, 2011 and Raiet**

Corresponding author:
e-mail: habostash@gmail.com

al., 2016). The production of mesoporous Silica - AgNPs is relatively inexpensive and the addition of these particles into goods such as plastics, clothing, creams, and soaps increase their market value (**Fenget *al.*, 2000**).

The aim of the work presents an overview of mesoporous silica-silver nanoparticles preparation by chemical methods and the implications of their use in controlling pathogenic microbes as they were tested for their antibacterial efficacy for different multidrug-resistant bacterial strains.

Materials and Methods

Chemicals

PluronicP123 (triblockcopolymer P123, EO₂₀PO₇₀EO₂₀, Mw of \approx 5800), tetraethyl orthosilicate (TEOS, \geq 99.0%), 3-Aminopropyltrimethoxysilane (APTS, 97%), 2,4,6-trinitrobenzenesulfonic acid (TNBS, 1 M in H₂O), potassium tetraboratetetrahydrate (K₂B₄O₇, \geq 99.5%), tetrabutylammoniumbromide (\geq 98%), 1-butanol (\geq 99%), HCl (35wt. %), hydrazine hydrate, silver acetate(99.99%), 1,2,4-trimethylbenzene solvents including methanol and ethanol were purchased from Sigma-Aldrich and used without further purification.

Synthesis of High Valence of Mesoporous Silica Silver Nanoparticles

The KIT-6 was synthesized as reported by **Qianet *al.* (2012)** and **Hassan *et al.* (2016)** with some modification. Ten g of PluronicP123 were melted (75°C) and then dissolved in 300 ml distilled water and 35 ml HCl (35 wt. %). The mixture was sheared at 350 rpm for 1 h. at 35°C then, 10 ml of 1-butanol and 1 ml of 1, 2,4-trimethylbenzenewere added at once to the stirred mixture for 30 min. at 35°C. After that, 20 g of TEOS was added to the stirred mixture and it was further stirred for 24 h. at 35°C. Then, the mixture was transferred to 500 ml Teflon autoclave and the hydrothermal process was carried out for 48 h. at 130°C under static conditions. The dried obtained white material after filtration and washing with mixture of water and ethanol was finally calcined in air atmosphere at 600 °C for 8h.

The obtained free surfactant KIT-6 was coupled with APTS to functionalize the KIT-6 pores with propylaminemoieties as following, 2.0 g of APTS was added directly to 5.0 g of degassed KIT-6 in 150 ml dry toluene under mechanical stirring for 4 h, at ambient temperature and then refluxed for another 12 h. The obtained material NH₂-KIT-6 was recovered by centrifuge, washed several times with ethanol- water mixture (50/50 V/V) to remove unreacted APTS molecules and vacuum dried at 60°C overnight (**Hassan *et al.*, 2014**).

The amino groups functionalized KIT-6 was determined gravimetrically by using, 2, 4, 6-trinitrobenzenesulfonic acid (**Weber *et al.*, 2000**). The degassed NH₂-KIT-6 (0.1 g) was suspended in double distilled water (1 ml) at 50°C for 2 h and left to cool. Then, the suspended NH₂-KIT-6 was further diluted with 5 ml of 100 mmol

Corresponding author:
e-mail: habostash@gmail.com

borate buffer ($K_2B_4O_7$; pH=9.3), and 1.5 ml of 1000 mmol TNBS solution was added and allowed to react for 4 h at 35 °C. After that, the NH_2 -KIT-6 was recovered by centrifuge at 14000 rpm for 5 min. The supernatant absorption was measured at 350 nm to determine the concentration of TNBS molecules. Reference samples were prepared in parallel composed of 6 ml of double distilled water of $K_2B_4O_7$ material without NH_2 -KIT-6 material, and the concentration of amino was confirmed with TNBS solutions.

The doping of silver nanoparticle (AgNPs) on NH_2 -KIT-6 at different loading was prepared in dry toluene using tetrabutylammonium bromide as cationic surfactant and silver acetate as a silver precursor. Briefly, 1.0 g of NH_2 -KIT-6 (1.628 mmol of $-NH_2$) was suspended in 10 ml of toluene under ultrasonic irradiation for 15 min, and 5 ml of aqueous containing 0.25% tetrabutylammonium bromide and 6 μ l of hydrazine are added and the mixture was further sonicated for additional 5 min. A 0.138 g (0.81 mmol) of silver acetate in 5 ml of distilled water was injected into the sonicated mixture under vigorous stirring. The mixture color slowly turned from white to pink, ruby and dark red color, confirming formation of AgNPs. The mixture temperature is raised to 45°C to ensure the compellation of reaction for 2 h, and the solvents were drained under vacuum at 80°C. After solidification, the obtained sample was washed several times with water-ethanol (90/5; V/V) until free tetrabutylammonium bromide was detected by $AgNO_3$. Finally, the obtained sample was dried under vacuum for 6 h. AgNPs immobilized in NH_2 -KIT-6 was stirred in 10 % HNO_3 and analyzed by Inductive Coupled Plasma (ICP). The samples were donated as Ag/ NH_2 -KIT-6(x), where x represents the weight ratio of Ag^0 immobilized on NH_2 -KIT-6 3.2 and 7.1 %.

Characterization of Mesoporous Silica Silver Nanoparticles

The XRD patterns were performed in X'Pert PRO instrument using $Cu K\alpha$ radiation at 40 kV and 30 mA. In powder XRD patterns, the positions of the peaks are determined only by the dimensions and shape of the unit cell (**McCusker and Baerlocher, 2001 and Rai and Duran, 2011**) and in general the intensities depend on the type of atoms and their position within the unit cell. Diffractograms were obtained from 0.5 to 10 (2θ) at a scanning speed of 0.05 deg. min^{-1} and counting time of 5s.

The N_2 -adsorption isotherms were performed at -196 °C in NOVA 3200 system instrument. The specific surface area was measured by applying the BET equation to the adsorption isotherm in regime ≥ 0.35 of P/P_0 value. The pore sizedistribution was calculated from Barrett–Joyner–Halenda (BJH) method. The total pore volume was considered to be the volume of liquid N_2 adsorbed at a relative pressure of 0.98. Prior to the analysis, the samples were outgassed under vacuum at 140°C for at least 16 h. High Resolution Transmission Electron Microscope images were obtained on a JEOL JEM 2100 microscope. Transmission Electron Microscope

Corresponding author:
e-mail: habostash@gmail.com

samples were prepared by sonication of the powder in ethanol and evaporating one drop onto a holey carbon film.

The FTIR spectra were recorded on a Nicolet iS10 Fourier transform infrared spectrophotometer. X-ray photoelectron spectroscopy (XPS) was carried out using a Thermo Scientific K-ALPHA USA instrument equipped with a dual X-ray source, using the AlK α radiation anode and a hemispherical energy analyzer. With an analyzer chamber pressure of 10⁻⁹torrat a power of 250W. Metal' s concentration impregnated in the samples was quantitatively determined using standard methods of analyses including Inductive Coupled Plasma (ICP). The ICP instrument is ICP-OES Perkin-Elmer Optima 2000DV.

Microbiological Experiments

Bacterial Cultures

Two Pathogenic bacterial strains, Gram negative *Pseudomonas aeruginosa*(ATCC9027) and Gram positive *Staphylococcus aureus*(ATCC43300) obtained from American type (ATCC,US) culture collection were used in this study. During the experimental period, the cultures were grown on nutrient agar and maintained at 4°C. For long term preservation, the cultures were stored in vial tubes containing 1ml aliquots plus 20% glycerol at -20°C(EL-Batalet *al.*, 2013). Bacterial cultures at the log phase of growth were prepared in nutrient broth after 16 h. of incubation at37°C.

Antibacterial Susceptibility Testing

Eight different antibiotics including Cefodizime (CFZ) 30 μ g, Cefoperazone (CEP) 75 μ g, Streptomycin (S) 10 μ g, Chloramphenicol (C) 30 μ g, Neomysin (N) 30 μ g, Sulfamethoxazole-trimethoprim (SXT) 25 μ g, Nalidixicacid (NA) 30 μ g and Colifuran (F) 200 μ g as standard antibacterial agents were used and antibacterial susceptibility test was performed by disk diffusion method on Mueller–Hinton agar plates according to Kheirallaet *al.*(2014).

Assessment of the Antibacterial Activity of Mesoporous Silica Silver Nanoparticles

The antimicrobial efficacy of silver nanoparticles with different concentrations (3.2 and 7.1%) was tested against *Pseudomonas aeruginosa*and *Staphylococcus aureus*by:

a- Well DiffusionTest:

Plates of Mueller–Hinton agar were inoculated using a sterile swab to produce a confluent lawn of growth. Using sterile cork borer, the well (6 mm) was made into

Corresponding author:
e-mail: habostash@gmail.com

each Petri dish. A 50 μ l of (Ag/ NH₂-KIT-6(x), 100 μ g/ml) suspended into dimethyl sulfoxide (DMSO) was put into the wells, and then the plates were left at refrigerator for 3 hours to allow diffusion of the test sample. The plates were incubated for 18-24 h. at 37°C and the inhibition zones were measured, (DMSO) was used as a negative control according to **Iconaru et al. (2012)**.

b- Minimum Inhibitory Concentration (MIC) and Minimum Bactericidal Concentration (MBC) Test:

The minimum inhibitory concentration and MBC of silver nanoparticles were assessed by the macro dilution broth susceptibility test according to the method based on the US National Committee for Clinical Laboratory Standards Guidelines, with modifications incorporated for nanomaterials by **Karthikeyan et al. (2011)** and **Kheiralla et al. (2014)**. Sterile Mueller–Hinton broth was used as diluents for the preparation of silver nanoparticles dilution. A serial dilution of the 0.01mg/ml silver nanoparticles solution was prepared within a desired range. One milliliter of each bacterial suspension that was prepared by suspending colonies from an overnight cultured tested bacteria on nutrient agar in sterile saline solution (0.85% NaCl) and adjusting turbidity to 0.5 McFarland (2×10^6 CFU/ml) was inoculated and then tubes were incubated for 24 h. at 37°C, the control tubes without the silver nanoparticles were assayed simultaneously. Minimum inhibitory concentration is the lowest concentration of antimicrobial agents that inhibited 90 percent of the bacterial growth was examined visually by checking the turbidity of the tubes. To test the bactericidal effect a loopful from each tube was inoculated on Mueller–Hinton agar and incubated for 24 h. at 37°C. The nanoparticles concentration causing bactericidal effect was selected based on absence of colonies on the agar plate (**Ruparelia et al., 2008**). The results were plotted as the mean value of 3 mutually independent experiments.

Action of Mesoporous Silica Silver Nanoparticles on the Ultrastructure of Bacterial Cells

The effects of Ag/NH₂-KIT-6(x) on the morphology of both *P. aeruginosa* and *S. aureus* were examined under transmission electron microscopy (TEM). Cells of *P. aeruginosa* and *S. aureus* before and after treatment with certain concentration of AgNPs representing the MIC for each were fixed overnight with 2.5% glutaraldehyde. Samples were post-fixed in 2% osmium tetroxide, dehydrated in an ascending series of graded ethanol, infiltrated and embedded in spur resin. Then, ultra-thin sections (60 nm thicknesses) were cut using ultra -microtome stained with uranyl acetate and counter-stained with 4% lead citrate. These sections were mounted on carbon-coated copper grids and observed under TEM (JEOL1010) (**Grigor'eva et al., 2013**).

Corresponding author:
e-mail: habostash@gmail.com

Statistical analysis

The experiments were replicated three independent times and the data are presented as mean \pm STD. Statistical analysis was carried out using Student's t test. Differences were considered statistically significant when P-value was less than 0.01.

After testing the data for normality, the differences in the treatments were tested using one-way analysis of variance (ANOVA 1) according to SPSS software (SPSS, 2006). A post-hoc test was applied when differences were significant.

Results and Discussion

Overuse or misuse of antimicrobial agents has led to the development of multi-drug resistant bacteria. To overcome the limitations of conventional synthetic antimicrobial compounds, nanotechnology represents an alternative strategy in developing alternative antimicrobial agents that can efficiently kill bacterial cells and display immense potential for use in both medical and veterinary applications (Yuan *et al.*, 2017).

Characterization of Mesoporous Silica Silver Nanoparticles

The sol-gel technique is one of the most important facile methods for porous preparation materials. The ordered cubic pore of silicate was synthesized using TEOS as silica precursor, HCl as a hydrolysis catalyst, P123 as structure directing agent (PO moieties as phase separation inducers; PEO moieties as a gelling agent) and butanol as co-surfactant. The pore construction morphology is determined by the balance between the silica coarsening and the structure freezing by P123 and butanol-co-surfactant that create the cubic morphology of the obtained monolithic silica. The second phase includes grafting of APTS on the silica in toluene, forming covalent bond between the monolithic silica and amino-organosilane moieties (Fig. 1). After that, the obtained amino-silicate (NH₂-KIT-6) was used as a platform to cap the reduced silver nanoparticle. In this stage, the silver acetate was embedded on NH₂-KIT-6, forming an Ag-NH₂-SiO₂ complex, and an appropriate amount of hydrazine was used to promote the reduction of the silver complex.

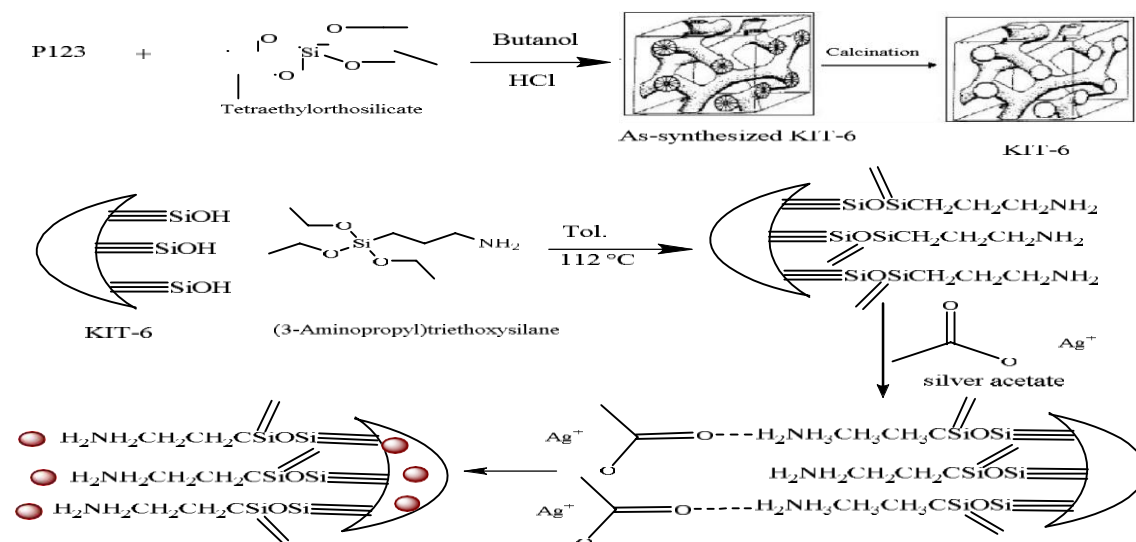


Fig.1: Schematic representation of the preparation of KIT-6, NH₂-KIT-6 and Ag/NH₂-KIT6(x).

The concentration of amino group per gram was of 1.45 mmol g⁻¹ and the immobilized silver according to ICP analysis was of 7.1% and 3.2%, for Ag/NH₂-KIT-6(7.1 %) and Ag-NH₂-KIT-6(3.2%). The FTIR assembly details of the KIT-6 functionalized NH₂-KIT-6 and Ag/NH₂-KIT-6(x), were examined. Spectra of NH₂-KIT-6 and Ag immobilized on Ag-NH₂-KIT-6(1.7&3.2) are shown in **Fig. 2** The KIT-6, NH₂-KIT-6 and Ag/NH₂-KIT-6 (7.1 and 3.2 %) exhibit the characteristic stretching broad bands associated with ≡Si-OH groups in the regime of 3450–3350 cm⁻¹, while the corresponding binding band for KIT-6 & NH₂-KIT-6, are observed at 1665 cm⁻¹ and 1650 cm⁻¹ for Ag/NH₂-KIT-6. The NH₂-KIT-6 exhibits the characteristic -CH₂ asymmetric and symmetric stretching bands near 2933 cm⁻¹ and 2821 cm⁻¹, respectively. While asymmetric Si-O-Si stretching bands appeared near 1066 cm⁻¹, the band near 969 cm⁻¹ is due to the Si-O bending in the Si-OH groups and asymmetric Si-O-Si stretching band appeared near 810 cm⁻¹. The vibration band at 3137 cm⁻¹ in NH₂-KIT-6 is attributed to the stretching vibration of -NH₂ that is in hydrogen bonding with Si-OH. The presence of asymmetric -N-H bending vibration near 707 cm⁻¹ confirms the incorporation of an amino group on the KIT-6 material. The band at 1380 cm⁻¹ associated with -CH₂ vibration, can be seen for the samples containing aminopropyl groups containing silver metal (Coates, 2000 and Wang *et al.*, 2005). However this band became more intense as Ag loading increase, implying free mobility of propylamine moieties after deposition Ag⁰ on -Si-OH.

Moreover, the significant reduction in band intensities at 3450–3350 cm⁻¹, conforming consumption of hydroxyl group after Ag anchoring in NH₂-KIT-6 surface, suggesting that portion of silver acetate is incorporated on -SiO₂ moieties. Finally, the intensity of the characteristic absorption bands in the range 1350–960

Corresponding author:
e-mail: habostash@gmail.com

cm^{-1} are also observed for all the samples, indicating slight changes in the pore structures after adsorption, which may be because of inherent disorder in the virgin and functionalized material structures (Sajabet *et al.*, 2011).

The low angle XRD patterns of KIT-6, NH_2 -KIT-6 and Ag/NH_2 -KIT-6 (3.2 and 7.1%) are shown in **Fig. 3**. The KIT-6 and NH_2 -KIT-6 samples exhibit three well-resolved; one strong intense diffraction peak and two minor diffraction peaks that assigned to (2 1 1), (2 2 0) and (3 3 2) reflections, which can be indexed to $\sqrt{3}d$, suggesting high ordered cubic mesoporous structure. It is clear that the intense peaks are shifted to lower angle after grafting APRTS molecule and more shift is noticed after Ag^+ loading. This behavior is resulted from increase the pore wall due to the grafting Ag^0 on propylaminemoieties. In addition, the a_0 (unit cell parameter) is increased after Ag^0 immobilization on KIT-6, escorted by the shift of the intense peak (2 1 1) reflection to lower angle. The high angle XRD patterns of KIT-6, NH_2 -KIT-6, Ag/NH_2 -KIT-6 (3.2, 7.1%), are shown in **Fig. 4**. The XRD patterns of KIT-6 and NH_2 -KIT-6 showed broad peak centered at 23.11° , while very weak peaks of the Ag^0 species in Ag/NH_2 -KIT-6 (3.2) materials is detected due to the high dispersion of silver on NH_2 -KIT-6, while four peaks at 38.04° , 44.29° , 64.30° and 77.39° corresponding to (1 1 1), (2 0 0), (2 2 0) and (3 1 1) plane-reflections of fcc Ag^0 nanostructure is noticed for Ag/NH_2 -KIT-6 (3.2%) material. The average particles size of AgNPs calculated from Scherrer's equation for (1 1 1)-plane were of 8 and 6.5 nm for Ag/NH_2 -KIT-6 (7.1%) and Ag/NH_2 -KIT-6 (3.2%), respectively.

The HRTEM images of the prepared samples are shown in **Fig. 5**. The KIT-6 and NH_2 -KIT samples exhibited well 3D cubic ordered mesoporous materials. The Ag^0 immobilized NH_2 -KIT showed ordered/disordered mesopores, however the irregular domains become predominant as Ag^0 loading increased due to the significant adsorption of Ag^0 particle on amino or silanol groups. Moreover, the AgNPs appeared highly dispersed on NH_2 -KIT and took the direction of KIT-6 pores, and the particle size distribution of AgNPs was of 4-9 nm size.

The N_2 adsorption-desorption isotherms of KIT-6, NH_2 -KIT-6 and Ag/NH_2 -KIT-6 (3.2, 7.1%) materials are shown in **Fig. 6** and the textural properties are collected in **Table 1**. All samples displayed Type IV isotherms with pronounced capillary condensation at high relative P/P_0 and H1 hysteresis loop, indicating large uniform channel-like mesoporous with narrow pore size distribution. The BET of KIT-6 was of $705 \text{ m}^2\text{g}^{-1}$, however, after grafting APRTS, the surface area decreased to $503 \text{ m}^2\text{g}^{-1}$, and the sharp decrease is noticed after immobilization of AgNP. The BET of Ag/NH_2 -KIT-6 (3.2, 7.1) was of $315 \text{ m}^2\text{g}^{-1}$ and $280 \text{ m}^2\text{g}^{-1}$, implying good dispersion of AgNP in the inter-connected pore of KIT-6.

The UV-Vis absorption of NH_2 -KIT and Ag/NH_2 -KIT-6 (3.2, 7.1) materials are shown in **Fig. 7**. The bare NH_2 -KIT didn't show any UV-Vis absorption, while Ag/NH_2 -KIT-6 (3.2%) and Ag/NH_2 -KIT-6 (7.1%) showed UV-Vis absorption at 413

Corresponding author:
e-mail: habostash@gmail.com

nmand 417 nm, respectively due to the Mie Plasmon resonance excitation of AgNP(Kim *et al.*, 2006). As the concentration of AgNP increased, the Plasmon resonance peak showed slight red shift, indicating the AgNP particle becomes larger somewhat. However, the low difference in AgNP particle size is attributed to the chemical coordination and steric effect of amino groups grafted on KIT-6 materials that obstruct the further growth of silver size.

The XPS spectra were used to demonstrate chemical environment for carbon, nitrogen and silver elements **Fig. 8** The high resolution XPS of C 1s is showed three peaks of binding energy at 284.28, 284.6 and 286.24 eV, appoint to C-C, C-H, and C-N sp^3 carbon, respectively. The XPS spectra in the N 1s binding energy ranged displayed the spin orbital single for NH_2 -KIT-6 and doublet for Ag/ NH_2 -KIT-6(7.1%) at 399.7 and 401.2 eV, indicating that electron transfer from nitrogen atom to metallic Ag^0 . These values are in agreement the presence of $-NH_2$ and coordinated $-NH_2$, as reported for other immobilized Ag^0 . The XPS profile of Ag 3d is curve-fitted into doublet spin-orbital with ≈ 6 eV separation, **Ferraria *et al.* (2010)** centered at 367.6 and 373.5 eV, which assigned to Ag $3d_{5/2}$ and Ag $3d_{3/2}$ present on NH_2 -KIT-6. In this study absence of the peaks at ~ 368 and ~ 374 eV indicates that all silver atoms are reduced(**Gebeyehu *et al.*, 2016**).

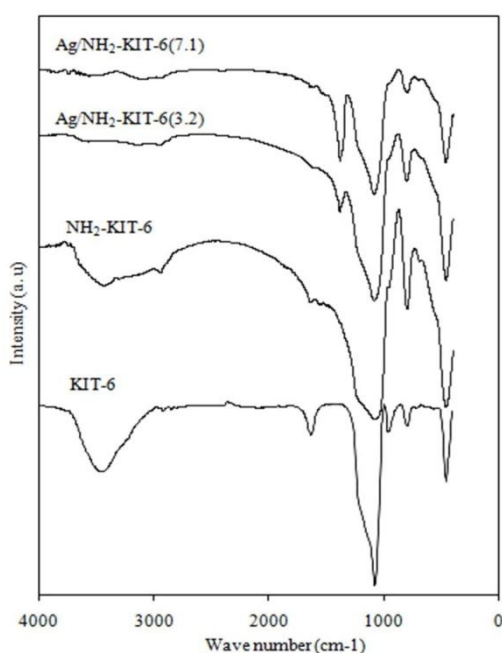


Fig. 2: FTIR spectra of calcined KIT-6, NH_2 -KIT-6, Ag/ NH_2 -KIT-6 (3.2 & 7.1%) materials.

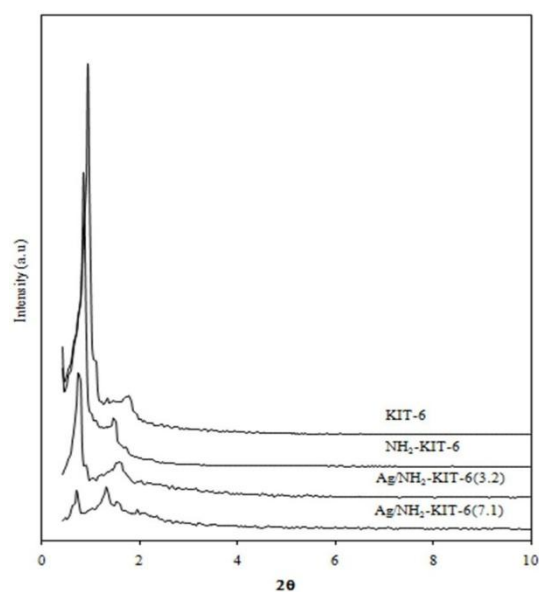


Fig. 3: Low XRD patterns for KIT-6, NH_2 -KIT-6 and Ag/ NH_2 -KIT-6 (3.2 & 7.1%) materials.

Corresponding author:
e-mail: habostash@gmail.com

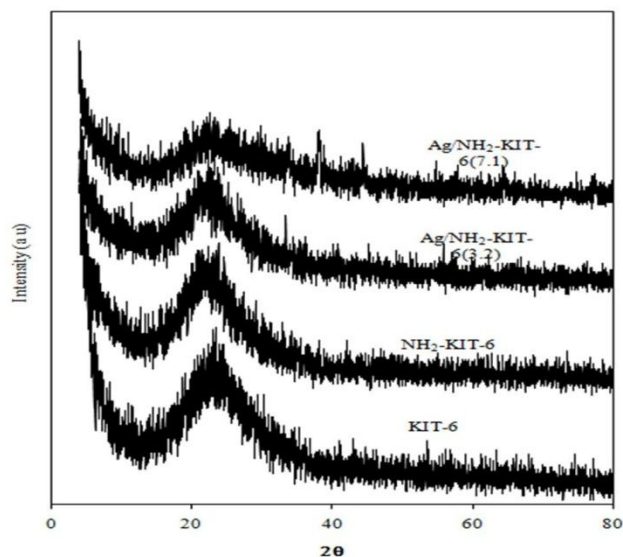


Fig. 4: High XRD patterns of KIT-6, NH₂-KIT-6 and Ag/NH₂-KIT 6 (3.2 & 7.1%) materials.

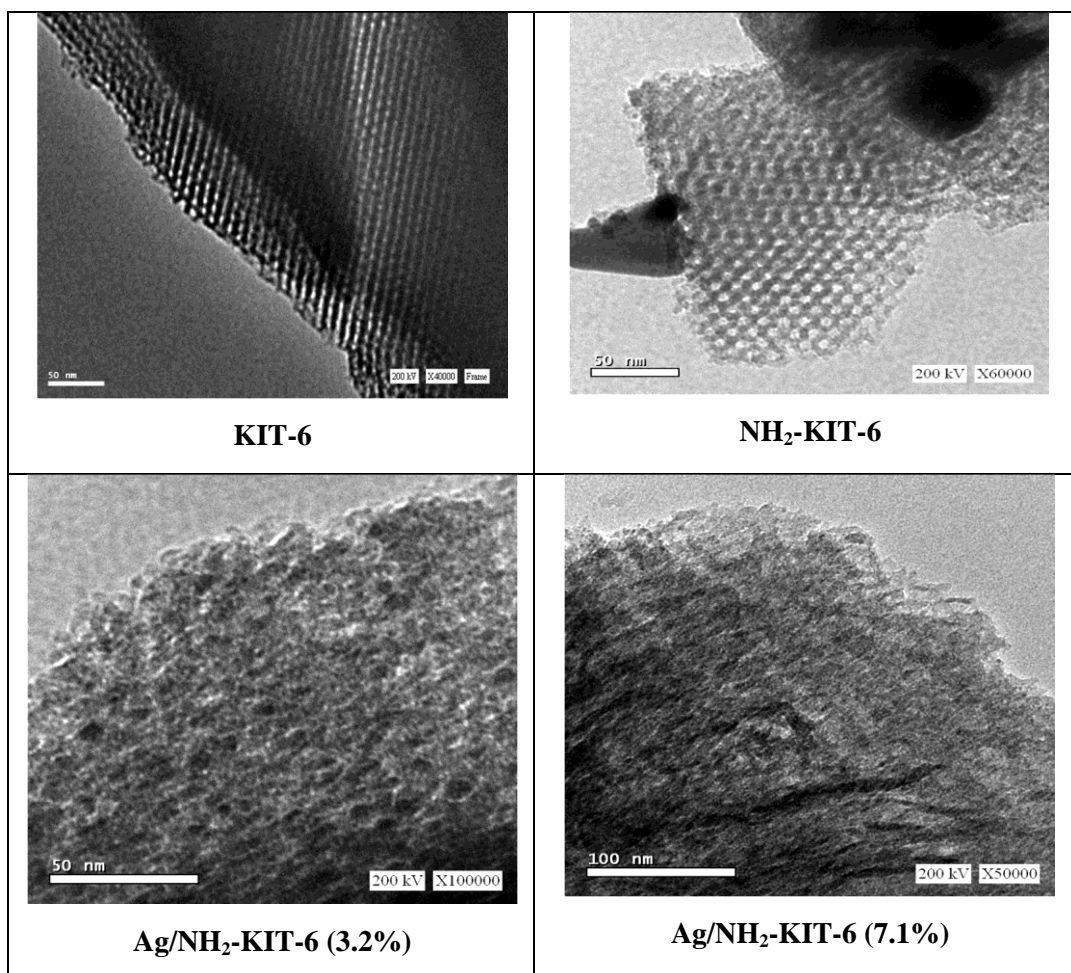


Fig. 5: High Resolution Transmission Electron Microscope images of KIT-6, NH₂-KIT-6 and Ag/NH₂-KIT-6 (3.2&7.1) materials.

Corresponding author:
e-mail: habostash@gmail.com

Table 1: The physicochemical characterization and textural of KIT-6, NH₂-KIT-6 and Ag/ NH₂-KIT-6 (3.2 and 7.1%)

Sample	$d_{211}(\text{Å})$	a_0 (nm)	W_T	S_{BET}^a (m^2g^{-1})	D_p^b	$V_p(c)$ m^3g^{-1}
					(nm)	
KIT-6	93.87	22.99	2.735	705	8.76	0.889
NH ₂ -KIT-6	102.61	25.13	5.945	503	6.62	0.62
Ag/NH ₂ -KIT-6(3.2)	119.23	29.21	8.865	315	5.74	0.46
Ag/NH ₂ -KIT-6(7.1)	124.27	30.44	10.04	280	5.18	0.39

S_{BET} , specific surface area; D_p , pore diameter; W_T , pore wall thickness [$a_0/\sqrt{2}$, (where $\sqrt{a_0} = \sqrt{6} a$)]

^aValues obtained from XRD studies.

^bValues obtained from N₂ adsorption results.

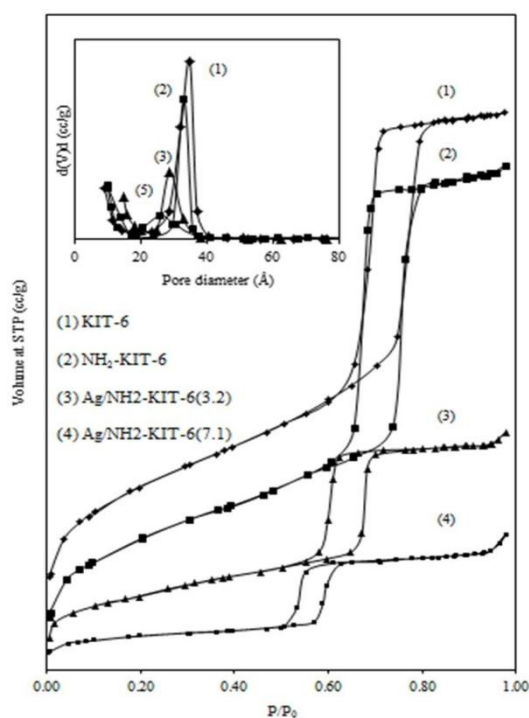


Fig. 6: Nitrogen adsorption/desorption and pore size distribution of KIT-6, NH₂-KIT-6 and Ag/NH₂-KIT-6 (3.2 & 7.1 %) materials.

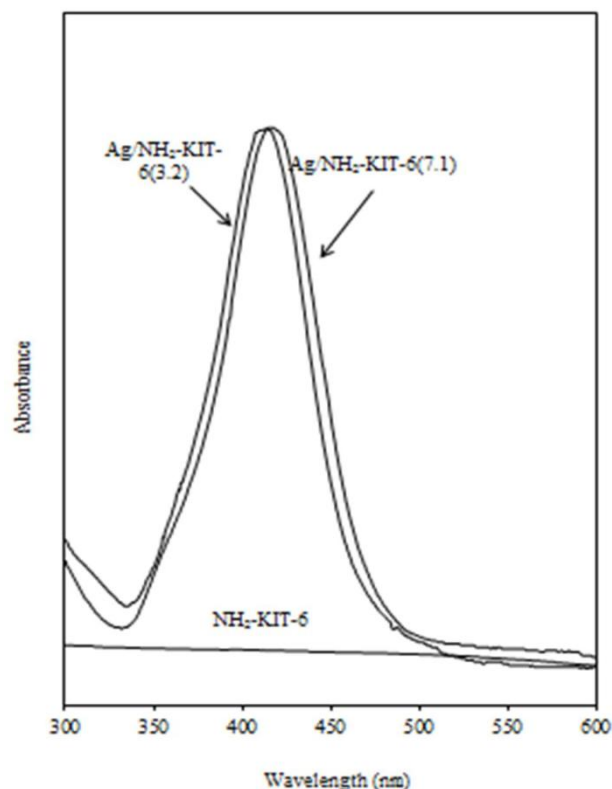


Fig. 7: UV-visible absorption spectra of NH₂-KIT-6, Ag/NH₂-KIT-6(3.2 & 7.1 %) materials.

Corresponding author:
e-mail: habostash@gmail.com

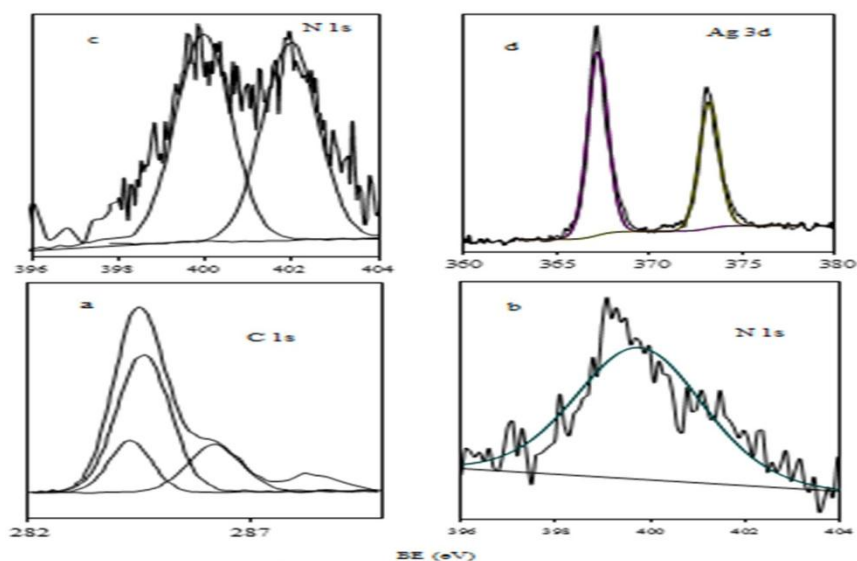


Fig. 8: XPS of **a:** C 1s, **b& c:** N 1s and **d:** Ag/NH₂-KIT-6 (7.1 %) material.

Antibacterial Activity

In vitro antibiotic susceptibility test was performed against two bacterial strains, *S. aureus* Gram positive & *Pseudomonas aeruginosa* Gram negative strains **Table 2**. *Pseudomonas aeruginosa* was found to be resistant to CFZ, NA and F while *S. aureus* was found to be resistant to NA and SXT. The antibacterial activity was affected with the concentrations 3.2 & 7.1% of Ag in Ag/NH₂-KIT-6(x). The maximum inhibition zone diameter obtained is 32 and 30 mm when using 7.1 % against *P. aeruginosa* and *S. aureus* respectively.

The present results showed that the mesoporous Ag/NH₂-KIT-6(x) exhibited good antibacterial activity and inhibited the growth of *P. aeruginosa* and *S. aureus* effectively. Whereas the mesoporous silica-KIT-6 and NH₂-KIT-6 exhibited no bacterial inhibitory effects due to the absence of metal silver nanoparticles in the composite material. APTS modification procedure plays a very important role in the immobilization of silver nanoparticles onto mSiO₂. Because the amino group of APTS could absorb a larger amount of Ag⁺ ions tightly through the complex and electrostatic interactions between Ag⁺ ions and amino functional groups. However, there only a small amount of Ag⁺ ions could be absorbed onto mSiO₂ APTS modification and the created Ag nanoparticles could easily break away from the channels of mSiO₂ during the filtration and washing procedure (**Shenet *et al.*, 2014**). The synthesized AgNPs appeared to be highly dispersed on NH₂-KIT6 and took the direction of KIT-6 pores, and the particle size distribution of mesoporous AgNPs was of 4-9 nm. In general, for nanoparticles to be effective, their typical size should not be larger than 50 nm. More precisely, mesoporous silver nanoparticles with size between 10 and 15 nm have increased stability, biocompatibility and enhanced antimicrobial

Corresponding author:
e-mail: habostash@gmail.com

activity(Yacamanet *al.*, 2001). Some studies have revealed that the antibacterial action of AgNPs is more effective against *S. aureus* and *K.pneumoniae* when nanoparticles of smaller diameter (<30nm) are used (Collins *et al.*, 2010). The antibacterial effect of AgNPs as proposed is due to their smaller particles size that apparently has superior penetration ability into bacteria, especially in Gram-negative (Moroneset *al.*, 2005)

Antimicrobial efficacy of AgNPs was evaluated by many researchers against a broad range of microbes, including MDR and non-MDR strains of bacteria, fungi, and viruses (Malarkodiet *al.*, 2013). Nano-sized metal particles are now well-established as a promising alternate to antibiotic therapy because they possess unbelievable potential for solving the problem associated with the development of multidrug resistance in pathogenic microorganisms, hence also regarded as next-generation antibiotics (Raiet *al.*, 2012).

Table 2:Antibacterial activityof Ag/NH2-KIT-6(x) versus antibacterial activity of standardantibiotics against *S. aureus*and*P.aeruginosa*.

Antibacterial agent	Inhibition zone (mm)	
	<i>S. aureus</i>	<i>P. aeruginosa</i>
Ag/NH2-KIT-6 (7.1%)	30.0±0.0a	32.0±2.0a
Ag/NH2-KIT-6 (3.2%)	23.0±0.0bc	25.0±0.0b
Cefodizime(CFZ)	13.0±0.0d	0.0±0.0f
Cefoperazone(CEP)	29.0±1.0a	17.0±0.0d
Streptomycin(S)	23.0±0.0bc	20.0±0.0c
Nalidixi acid (NA)	0.0±0.0e	0.0±0.0f
Neomysin(N)	21.0±1.0bc	15.3±0.6e
Sulfamethoxazole-trimethoprim(SXT)	0.0±0.0e	17.0±0.0d
Chloramphenicol(C)	24.0±1.0b	17.0±0.0d
Colifuran(F)	18.7±8.1c	0.0±0.0f
F value	49.671***	843.590***

The antimicrobial activity of Ag /NH2-KIT-6 (x) was also evaluated using the macrodilution broth susceptibility method. MIC and MBC of silver nanoparticles shown best results with the concentration 7.1% of Ag/NH2-KIT-6 than the concentration 3.2% of Ag/NH2-KIT-6 (Table 3). The MIC and MBC for the Ag /NH2-KIT-6 (3.2%) against tested bacteria *P. aeruginosa*and *S. aureus*differ in their values, but MIC equals MBC at the concentration (7.1%).

The concentration ofAg/NH2-KIT-6 (7.1%) shows 0.0045 and 0.041µl/ml for both MIC and MBC against *P. aeruginosa*and *S. aureus*respectively, i.e.completely inhibited, which indicated that the MIC and MBC ofAg/NH2-KIT- 6(7.1%) are equal (Table 3). The obtained result agree with Ansari *etal.* (2011)

Corresponding author:
e-mail: habostash@gmail.com

whom showed that the AgNPs of 5–10 nm dimension display both bacteriostatic as well as bactericidal effects against *S. aureus*, MSSA and MRSA.

Gram-negative bacteria are more sensitive against nano Ag/NH₂KIT-6 than gram-positive bacteria, also **Klapiszewskiet al .(2015)** and **Yuan et al. (2017)** demonstrated that, AgNPs were more effective against Gram-negative *P. aeruginosa* than Gram-positive *S. aureus*, which could be explained by differences in membrane structure and the cell wall composition, which influence bacterial susceptibility to AgNPs.

Table 3: The MIC and MBC of mesoporous silver nanoparticles (Ag/NH₂-KIT-6 (3.2 and 7.1%) against *P. aeruginosa* and *S. aureus*.

Ag/NH ₂ -KIT-6 (x) (µg/ml)		Tested Bacterium	
		<i>P. aeruginosa</i>	<i>S.aureus</i>
3.2%	MIC	0.0045	0.041
	MBC	0.013	0.37
7.1%	MIC	0.0045	0.041
	MBC	0.0045	0.041

The electron micrographs of the surface structures by TEM of *P. aeruginosa* and *S. aureus* treated and untreated cells with Ag/NH₂-KIT-6(7.1%) are shown in **Fig 10**. The treated bacterial cells were significantly changed, and major damage was observed in the outer cell membrane. Nanoparticles that accumulated in the membrane as well as some penetrating the cells can also be discerned in the TEM micrograph.

A recent report has demonstrated the antibacterial activity of mesoporous silica silver nanoparticles on both Gram positive and Gram negative microbes. The mechanism of the antibacterial activity of mesoporous silica nanoparticles was attributed to the electrostatic interaction of phosphate groups on the microbial cell wall and the cationic head group of the mesoporous silica nanoparticles. Also, the organic tail region embeds itself in the lipid bilayer. This, in turn, leads to the free flow of electrolytes out of the microbe and causes the cell death. This is believed to be the mechanism of cell death (**Xia et al., 2009** and **Vithiya et al., 2014**).

Corresponding author:
e-mail: habostash@gmail.com

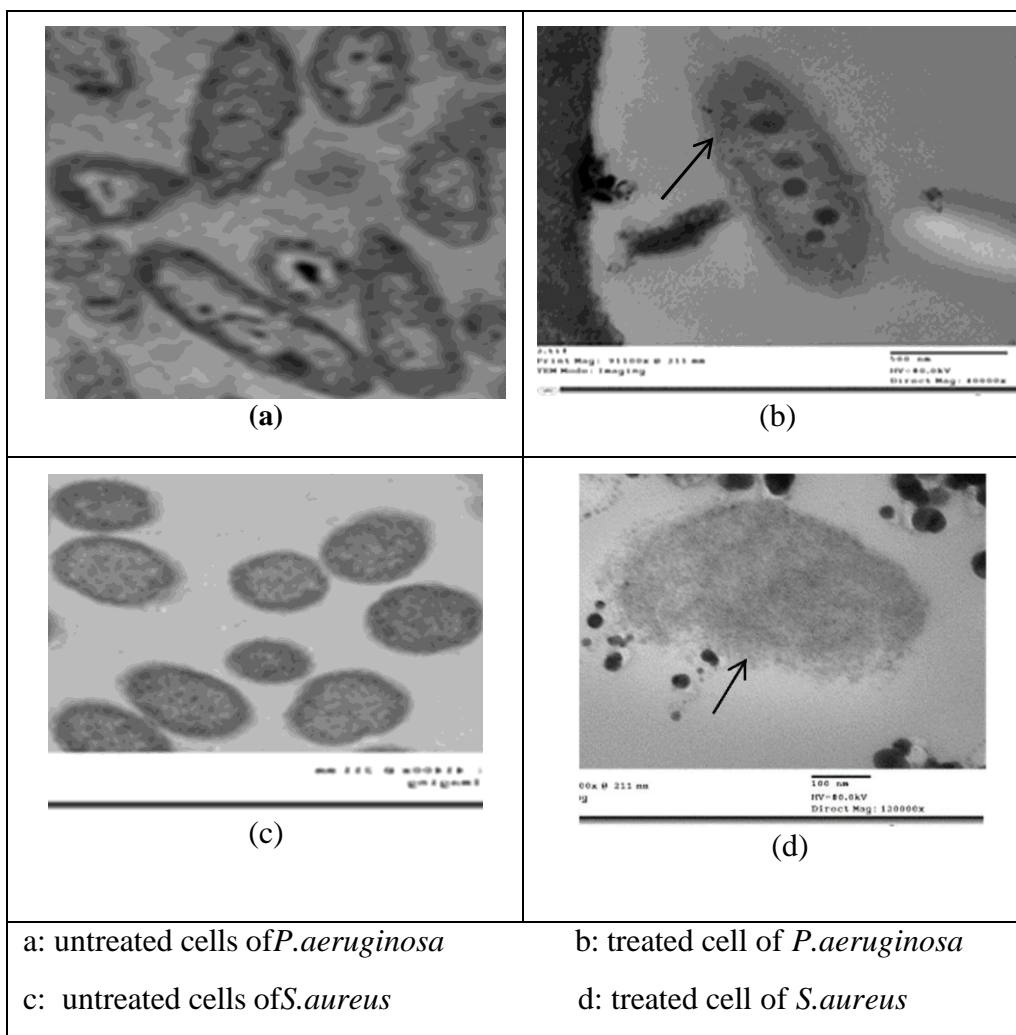


Fig. 10: TEM micrographs of the action of mesoporous Ag/NH₂-KIT-6 (7.1%) on the ultrastructure of *P. aeruginosa* and *S. aureus* cells.

Conclusion

In this study, antibacterial activity of mesoporous Ag/NH₂-KIT-6(x) nanoparticles synthesized using a chemical reduction method was tested against *P. aeruginosa* and *S. aureus*. The obtained results confirmed that different concentrations of mesoporous Ag/NH₂-KIT-6(x) nanoparticles have very strong inhibitory properties in comparison with standard antibiotics. Different degrees of sensitivity were shown among the bacteria, probably due to the difference in the structure and/or composition of their cell walls. These pathogens are very dangerous for human as it is associated with many systemic diseases. From TEM analysis it could be observed that when this interaction occurred, the mesoporous Ag/NH₂-KIT-6(x) nanoparticles were able to cause microbial cell membrane damage. It is wished that in near future using synthetic or purified forms of these mesoporous nanoparticles could be easily fight pathogenic microbes and improve health.

Corresponding author:
e-mail: habostash@gmail.com

References

- **Chen, M.; He, X.; Wang, K.; He, D.; Yang, S.; Qiu, P. and Chen, S. (2014):** A pH-responsive polymer/mesoporous silica nanocontainer linked through an acid cleavable linker for intracellular controlled release and tumor therapy *in vivo*. *J. Mater. Chem. B* **2**:428–36.
- **Coates, J. (2000):** Interpretation of infrared spectra: A practical approach, R. A. Meyers, ed., *Encyclopedia of Analytical Chemistry*, W. John & Sons Ltd, Chichester, pp.10815-10837.
- **Collins, T. L.; Markus, E. A.; Hassett, D. J. and Robinson, J. B. (2010):** The effect of a cationic porphyrin on *Pseudomonas aeruginosa* biofilms. *Curr. Microbiol.* **61**:411–416.
- **EL-Batal, A.I.; Amin, M.A.; Shehata, M.M.K. and Hallol, M. (2013):** Synthesis of Silver nanoparticles by *Bacillus stearothermophilus* using Gamma Radiation and their antimicrobial activity. *World Appl. Sci. J.* **22** (1):01-16.
- **Feng, Q.L.; Wu, J.; Chen, G.Q.; Cui, F.Z.; Kim, T.N. and Kim, J.O. (2000):** A mechanistic study of the antibacterial effect of Silver ions on *Escherichia coli* and *Staphylococcus aureus*. *J. Biomed. Mater. Res.* **4**:662-8.
- **Ferraria, A.M.; Boufi, S.; Battaglini, N.; Botelho do Rego, A.M. and Rei Vilars, M. (2010):** Hybrid systems of Silver nanoparticles generated on cellulose surfaces. *Langmuir*, **26**(3):1996-2001.
- **Franci, G.; Falanga, A.; Galdiero, S.; Palomba, L. ; Rai, M.; Morelli, G.; and Galdiero, M. (2015):** Silver nanoparticles as potential antibacterial agents. *Molecules*, **20**:8856-8874.
- **Gebeyehu, M.B.; Chang, Y. Abay, A.K.; Chang, S.; Lee, J.; Wu, C.; Chiang, T. and Murakami, R. (2016):** Fabrication and characterization of continuous silver nanofiber/polyvinylpyrrolidone (AgNF/PVP) core-shell nanofibers using the coaxial electrospinning process. *RSC Advances*, **6**(59): 54162-54168.
- **Grigor'eva, A.; Saranina, I.; Tikunova, N.; Safonov, A.; Timoshenko, N. and Rebrov, A. and Ryabchikov, E. (2013):** Fine mechanisms of the interaction of Silver nanoparticles with the cells of *Salmonella typhimurium* and *Staphylococcus aureus*. *Biometals*, **26**(3):479–488.
- **Hassan, H.M.A.; Saad, E.M.; Soltan, M.S.; Betiha, M.A.; Butler, I.S. and Mostafa S.I. (2014):** A Palladium (II) 4-hydroxysalicylidene Schiff-base complex anchored on functionalized MCM-41: An efficient heterogeneous catalyst for the epoxidation of olefins. *App. Catal. A.* **488**:148-159.

Corresponding author:

e-mail: habostash@gmail.com

- **Hassan, H.M.A.; Betiha, M.A.; Khder, S.; Mostafa, M. and Gallab, M. (2016):** Hafnium pentachloride ionic liquid for isomorphic and postsynthesis of HfKIT-6 mesoporous Silica: catalytic performances of Pd/SO₄²⁻/HfKIT-6. *J. Porous. Mater.* **23**: 1339-1351.
- **Iconaru, S.L.; Prodan, A.M.; Le Coustumer, P. and Predoi, D. (2012):** Synthesis and antibacterial and antibiofilm activity of Iron Oxide Glycerol nanoparticles obtained by coprecipitation method. *J. Chemist.* **2013(2013)**: 1-6.
- **Kheiralla, Z.M.H.; Rushdy, A. A.; Betiha, M.A. and Yakob N. A.N. (2014):** High-performance antibacterial of montmorillonite decorated with silver nanoparticles using microwave assisted method. *J. Nanopart. Res.* **16**:2560.
- **Kim, K.; Kim, H.S. and Park, H.K. (2006):** Facile method to prepare surface-enhanced-Raman-scattering-active Ag nanostructures on silica spheres. *Langmuir*, **22**:8083-8088.
- **Klapiszewski, L.; Rzemieniecki, T.; Krawczyk, M.; Malina, D.; Norman, M.; Zdarta, J.; Majchrzak, I.; Dobrowolska, A.; Czaczyk, K. and Jesionowski, T. (2015):** Kraft lignin/silica-AgNPs as a functional material with antimicrobial activity. *Colloids. Surf. B Biointerfaces*, **134**:220-228.
- **Klevens, R.M.; Morrison, M.A.; Nadle, J.; Petit, S.; Gershman, K.; Ray, S.; Harrison, L.H.; Lynfield, R.; Dumyati, G. and Townes, J.M.(2007):** Invasive methicillin-resistant *Staphylococcus aureus* infections in the United States. *JAMA*. **298**:1763–1771.
- **Han, F.; Bai, Y.; Lin, R.; Yad, B.; Qi, Y.; Lun, N. and Zhang, J. (2011):** Template-Free Synthesis of Interconnected Hollow Carbon Nanospheres for High-Performance Anode Material in Lithium-Ion Batteries. *Adv. Energy Mater.* **1(5)**:798-801.
- **Malarkodi, C.; Rajeshkumar, S.; Paulkumar, K.; GnanaJobitha, G.; Vanaja, M. and Annadurai, G. (2013):** Biosynthesis of semiconductor nanoparticles by using sulfur reducing bacteria *Serratianematodiphila*. *Adv. Nano. Res.* **1**:83–91.
- **McCusker, L. B. and Baerlocher, C. (2001):** In introduction to Zeolite Science and practice, H.VanBekum, E. M. Flanigen, P. A. Jacobs, and J. C. Jansen, eds. Amsterdam: Elsevier, pp. 137,37.
- **Morones, J. R.; Elechiguerra, J. L.; Camacho, A.; Holt, K.; Kouri, J. B.; Ramírez, J. T. andYacaman, M. J. (2005):** The bactericidal effect of silver nanoparticles. *Nanotechnology*, **16**:2346–2353.

Corresponding author:
e-mail: habostash@gmail.com

- **Natarajan, S. K. and Selvaraj, S. (2014):** Mesoporous Silica nanoparticles: importance of surface modifications and its role in drug delivery. *RSC Adv.* **4**: 14328–14334.
- **Qasim, M.; Ananthaiah, J.; Dhara, S.; Paik, P. and Das, D. (2014):** Synthesis and characterization of ultra-fine colloidal Silica nanoparticles *Adv. Sci. Eng. Med.* **6**:965–973.
- **Qian, L.; Ren, Y.; Liu, T.; Pan, D.; Wang, H. and Chen, G. (2012):** Influence of KIT-6's pore structure on its surface properties evaluated by inverse gas chromatography. *Chem. Eng. J.* **213** :186-194.
- **Rai, M. and Duran, N. (2011):** Metal nanoparticles in microbiology, Springer-Verlag. Berlin Heidelberg.
- **Rai, M.K.; Deshmukh, S.D.; Ingle, A.P. and Gade, A.K. (2012):** Silver nanoparticles: The powerful nanoweapon against multidrug-resistant bacteria. *J. Appl. Microbiol.* **112**:841–852.
- **Rai, M.; Deshmukh, S.D.; Ingle, A.P.; Gupta, I.R.; Galdiero, M. and Galdiero, S. (2016):** Metal nanoparticles: The protective nanoshield against virus infection. *Crit. Rev. Microbiol.* **24**(1):46-56.
- **Karthikeyan, R.; Amaechi, B.T.; Rawls, H.R. and Lee, V.A. (2011):** Antimicrobial activity of nanoemulsion on cariogenic *Streptococcus mutans*. *Arch. Oral Biol.* **56**:437–445.
- **Ruedas-Rama, M. J.; Walters, J. D.; Orte, A. and Hall, E. A. H. (2012):** Fluorescent nanoparticles for intracellular sensing: A review. *Anal. Chim. Acta*, **751**:1–23.
- **Ruparelia, J. P.; Chatterjee, A. K.; Duttagupta, S. P. and Mukherji, S. (2008):** Strain specificity in antimicrobial activity of Silver and Copper nanoparticles. *Acta Biomater.* **4**(3):707-716.
- **Sajab, M.S.; Chia, C.H.; Zakaria, S.; Jani, S.M.; Ayob, M.K.; Chee, K.L.; Khiew, P.S. and Chiu, W.S. (2011):** Citric acid modified kenaf core fibres for removal of methylene blue from aqueous solution. *Bioresour. Technol.* **102**: 7237-7243.
- **Shen, Q. J.; Wang, H.; Yang, X.; Ding, Z.; Luo, H.; Wang, C.; Pan, J.; Sheng, and Cheng, D. (2014):** *J. Non-Cryst. Solids*, **391**:112–116.
- **SPSS (2006).** *SPSS base 15.0 User's guide.* SPSS inc., Chicago, USA.
- **Sweet, M.J. and Singleton, I. (2011):** Silver nanoparticles: A microbial perspective. *Adv. Appl. Microbiol.* **77**:115–133.

Corresponding author:
e-mail: habostash@gmail.com

- **Taraszkiewicz, A.; Fila, G.; Grinholc, M. and Nakonieczna, J. (2012):** Innovative strategies to overcome biofilm resistance. *Biomed. Res. Int.* **2013 (2013):**1-13.
- **Walker, B.; Barrett, S.; Polasky, S.; Galaz, V.; Folke, C.; Angstroms G.; Ackerman, F.; Arrow, K.; Carpenter, S.; Chopra, K.; Daily, G.; Ehrlich, P.; Hughes, T.; Kautsky, N.; Levin, S.; Maler, K.G.; Shogren, J.; Vincent, J.; Xepapadeas, T. and de Zeeuw, A. (2009):** Environment. Looming global-scale failures and missing institutions. *Science*, **325:**1345–1346.
- **Wang, X.; Tseng, Y.; Chan, J.C.C. and Cheng, S. (2005):** Catalytic applications of aminopropylated mesoporous Silica prepared by a template-free route in flavanones synthesis. *J. Catal.* **233:**266-275.
- **Weber, C.; Coester, C.; Kreuter, J. and Langer, K. (2000):** Desolvation process and surface characterisation of protein nanoparticles. *Int. J. Pharm.* **194:** 91-102.
- **Wu, S.; Mou, C. and Lin, H. (2013):** Synthesis of mesoporous silica nanoparticles. *Chem. Soc. Rev.* **42 :**3862–3875.
- **Xia, T.; Kovochich, M.; Liong, M.; Meng, H.; Kabehie, S.; George, S.; Zink, J.I. and Nel, A.E. (2009):** Polyethyleneimine coating enhances the cellular uptake of mesoporous silica nanoparticles allowed safe delivery of siRNA and DNA constructs. *ACS Nano.* **3(10):**3273-3286. **Vithiya, K.; Kumar, R. and Sen, S. (2014):** Bacillus sp. Mediated extracellular synthesis of silver nanoparticles. *Int. J. Pharm. Sci.* **6:**525-7
- **Yacaman, M. J.; Ascencio, J. A.; Liu, H. B. and Gardea-Torresdey, J. (2001):** Structure shape and stability of nanometric sized particles. *J. Vacuum. Sci. Technol. B. Microelectron. Nanometer. Struct.* **19:**1091–1103.
- **Yildirim, A.; Demirel, G. B.; Erdem, R.; Senturk, B.; Tekinay, T. and Bayindir, M. (2013):** Pluronic polymer capped biocompatible mesoporous Silica nanocarriers. *Chem. Commun.* **49:**9782–9784.
- **Yuan, Y.; Peng, Q. and Gurunathan, S. (2017):** Effects of Silver nanoparticles on multiple drug-resistant strains of *Staphylococcus aureus* and *Pseudomonas aeruginosa* from mastitis-infected goats: An alternative approach for antimicrobial therapy. *Int. J. Mol. Sci.* **18:**569.

Corresponding author:
e-mail: habostash@gmail.com

التأثير الميكروبي المضاد لجزيئات الفضة والسليكا المسامية النانوية على سلالات من البكتريا

المقاومة للمضادات الحيوية

¹سناء صبحي زكي ، ¹زينب محمد حسن خير الله ، ¹عبير احمد رشدي ، ¹حنان بشير ابوسطاش ، محمد احمد بطيحة²

١ - قسم النبات – كلية النبات للآداب و العلوم و التربية- جامعة عين شمس – أسماء فهمي – القاهرة – مصر

٢ - معهد بحوث البترول – القاهرة- مصر

الخلاصة

تم دراسة النشاط الميكروبي لجزيئات mesoporous Ag/NH₂-KIT-6(x) النانوية المخلقة بطريقة الأختزال الكيميائي ضد سلالتين من البكتريا هما *P.aeruginosa* و *S.aureus* وأكدت النتائج المتحصل عليها القدرة الهائلة لجزيئات Ag/NH₂-KIT-6(x) النانوية بمختلف تركيزات الفضة بها على تثبيط النمو الميكروبي لكلا من *S.aureus* و *P.aeruginosa* مقارنة بالمضادات الحيوية التي تم إستخدامها.

كما لوحظ وجود إختلاف فى درجة حساسية كلا الميكروبين للجزيئات النانوية وربما يعود هذا إلى إختلاف تركيب الجدر الخلوية لكلا منهما ولهذه الميكروبات أهمية كبيرة حيث أنها من أهم الميكروبات الممرضة للإنسان لإرتباطها بالعديد من الأمراض الجهازية ويتضح من صور الميكروسكوب النافذ مدى التلف التى أحدثته جزيئات Ag/NH₂-KIT-6(x) النانوية للأغشية الخلوية.

نأمل فى المستقبل القريب إستخدام أنواع مخلقة ونقية من الجزيئات النانوية فى صورة mesoporous لمواجهة الميكروبات الممرضة للإنسان.